Solar and Stellar Magnetic Fields: Origins and Manifestations
Proceedings IAU Symposium No. 354, 2019
M. Jardine, A. Kosovichev & K.G. Strassmeier, eds.

DOI: 00.0000/X000000000000000X

Analysis of the chromosphere and corona of low-activity early-M dwarfs.

Gaetano Scandariato[1], E. González Álvarez[2,3], J. Maldonado[2], A. Suárez Mascareño[4,5], M. Perger[6,7], and the HADES collaboration

[1]INAF - Osservatorio Astrofisico di Catania,
via S. Sofia 78, 95123 Catania, Italy
email: gaetano.scandariato@inaf.it

[2]INAF – Osservatorio Astronomico di Palermo, Piazza del Parlamento, 1, I-90134, Palermo, Italy,
[3]Dipartimento di Fisica e Chimica, Università di Palermo, Piazza del Parlamento 1, I-90134 Palermo, Italy,
[4]Instituto de Astrofísica de Canarias, 38205 La Laguna, Tenerife, Spain
[5]Universidad de La Laguna, Dpto. Astrofsica, 38206 La Laguna, Tenerife, Spain
[6]Institut de Cincies de lEspai (ICE, CSIC), Campus UAB, C/ Can Magrans, s/n, 08193 Bellaterra, Spain
[7]Institut d'Estudis Espacials de Catalunya (IEEC), 08034 Barcelona, Spain

Abstract. While most of the exoplanets have been found orbiting around solar-type stars, low-mass stars have recently been recognized as ideal exo-life laboratory. Currently, stellar activity is one of the limiting factors for the characterization of Earth-twins and for assessing their habitability: understanding the activity of M dwarfs is thus crucial. In this contribution I present the spectroscopic analysis of the quiet early-M dwarfs monitored within the HADES (HArps-n red Dwarf Exoplanet Survey) radial velocity survey. The spectra allow us to analyze simultaneously the Ca II H&K doublet and the Hydrogen Balmer series, while the intensive follow up gives us a large number of spectra ($\lesssim$100) for each target. We complement this dataset with ground-based follow-up photometry and archival X-ray data. I present our results on the activity-rotation-stellar parameters and flux-flux relationships, and discuss the correlation of emission fluxes at low activity levels and the evolution timescales of active regions.

Keywords. stars: activity, stars: atmospheres, stars: chromospheres, stars: coronae,stars: late-type, stars: low-mass, brown dwarfs, stars: rotation,stars: spots

1. Introduction

Recent planet search programs have started to monitor samples of M dwarfs, as they are are extremely interesting for the discovery of Earth-like planets. As a matter of fact, M dwarfs represent ∼75% of the stars in the solar neighborhood (Reid et al. 2002; Henry et al. 2006). Moreover, for a number of observational constraints, the chances of finding a temperate rocky planet (i.e. a planet at a convenient density and distance from its host star such to have liquid water on its surface) increase as the stellar mass decreases. Such planets are said to be inside the habitable zone of their host stars. Still, habitability is not guaranteed simply by an assessment of the distance from the star; several other factors, such as stellar activity and the strength of the stellar magnetic field, may move and/or shrink the habitability zone of a star (see Vidotto et al. 2013, and references therein). Thus, it is crucial to better understand the activity of M dwarfs and how it can affect the circumstellar environment.

The term "stellar activity" refers to a large class of phenomena that, in stars with convective envelopes, are triggered by the reconfiguration of the surface magnetic field.

These phenomena are commonly classified as spots, plages, flares, or coronal holes, and they take place throughout the stellar atmosphere. The places where these phenomena take place are called "active regions" (ARs). In this contribution I will discuss the results of an extensive analysis of the stellar activity of a sample of low-activity M dwarfs, which have been selected and monitored for planet-search purposes and for which we have collected measurements of photospheric, chromospheric and coronal activity indicators. My discussion is based on a group of four papers which we have recently published (Maldonado et al. 2017; Scandariato et al. 2017; Suárez Mascareño et al. 2018; González-Álvarez et al. 2019) and which the reader is encouraged to check in order to obtain further details on our analysis.

2. The project, the stellar sample and the data

The HArps-N red Dwarf Exoplanet Survey project (HADES, Affer et al. 2016; Perger et al. 2016) is a collaborative program between the Global Architecture of Planetary Systems project† (GAPS, Covino et al. 2013), the Institut de Ciències de l'Espai (ICE/CSIC, IEEC), and the Instituto de Astrofísica de Canarias (IAC). The aim of the project is to monitor the radial velocities of a sample of low-activity M-type dwarfs and discover new exoplanets.

Within the HADES framework we have monitored 71 stars with spectral types ranging between K7.5V and M3V (corresponding to the ∼3400–3900 K temperature range). These stars were observed with the HARPS-N spectrograph (Cosentino et al. 2012) mounted at the Telescopio Nazionale Galileo. The spectrograph covers the 383–693 nm wavelength range with a spectral resolution of ∼115,000. HARPS-N spectra were reduced using the most recent version of the Data Reduction Software (DRS) pipeline (Lovis & Pepe 2007).

The targeted stars have been selected as favorable for planet search, by consequence the sample is biased towards low activity levels with some exceptions. The data analyzed in this paper have been collected over seven semesters, from September 2012 to February 2016, and for each star we collected up to ∼100 spectra. Affer et al. (2016) give further details on the target selection and Maldonado et al. (2016) describe the determination of the stellar parameters.

HARPS-N spectra have been flux calibrated by comparison with a low-resolution synthetic spectral library. The stars showing the minimum emission in the cores of the Ca II H&K lines (commonly used as a tracer of chromospheric activity) are selected as spectral templates with minimum contribution by chromospheric emission, accounting that they span the full range of effective temperature covered by our stellar sample. For each star, the corresponding "quiet" spectral template is selected as the one with the closest effective temperature. Finally the spectra are subtracted by the selected template, such to obtain the "chromospheric" spectrum. Fluxes of the Ca II H&K and the hydrogen Balmer line (from Hα to Hϵ) are extracted by integrating the residual spectrum over convenient wavelength ranges.

Optical UBVRI photometry has been collected simultaneously to the HARPS-N campaign in the framework of the EXORAP project. This project consists in the nightly follow up of our sample of M dwarfs with an 80 cm f/8 Ritchey-Chretien robotic telescope (APT2) located at Serra la Nave (+14.973 E, +37.692N, 1725 m a.s.l.) on Mt. Etna and operated by INAF-Catania Astrophysical Observatory. The main goal of this project is to provide optical differential light curves by which we can characterize the photometric variability and measure the stellar rotation period.

† `http://www.oact.inaf.it/exoit/EXO-IT/Projects/Entries/2011/12/27_GAPS.html`

With the purpose of complementing our analysis with the coronal activity, we searched the catalogs of the X-ray missions XMM-Newton, Chandra and ROSAT, following this order of preference. Even if ROSAT is older and less sensitive than the most recent X-ray observatories, it is still the main source of X-ray measurements since it covered all the sky. In total, we find X-ray counterparts for 37 stars in our selected sample.

3. Stellar rotation, activity cycles and ARs evolution timescale

We look for periodic variability in the time-series of measurements of indicators compatible with both stellar rotation and long term magnetic cycles. We compute the power spectrum using a Generalised Lomb Scargle (GLS) periodogram (Zechmeister & Kurster 2009) and, if there is any significant periodicity, we fit the data using a sine function with the detected period. Then we repeat the same process in the residuals of the fit. Typically this allowed us to determine the stellar rotation, and in some cases to unveil the presence of an activity cycle. Following this procedure we measure the rotation periods of 32 of the stars of our sample and identify magnetic cycles in 14 stars.

Stars in our sample are typically slow rotators, as we find an average rotation period of ∼30 days for early M-dwarfs and of ∼80 days for mid M-dwarfs. This is consistent with the fact that our sample is biased towards low activity levels, which correspond to slow rotation rates. As a matter of fact, in Fig. 1 we show that the rotation period of stars in our sample strongly anti-correlates with the R'_{HK} activity index. This trend is consistent with other samples of M dwarfs previously analyzed.

Cycle lengths are typically of a few years, with the longest cycles detected at almost 14 years. For the cycle measurements we are limited by the time-span of the survey. Cycles longer than ∼3–4 years are not measurable by our campaign on its own, they always require support data (previous HARPS spectra or ASAS photometry). There is a hint of a lower envelope of the distribution of cycle lengths against the color B-V (hence, the stellar mass) which might indicate that lower mass stars have longer magnetic cycles (Fig. 1).

We analyze the same data using the Pooled Variance (PV) approach (Donahue et al. 1997a). The PV measures the average variance in the data over a given time bin τ running along the series of measurements. When τ increases, the PV remains constant until the effects from processes with longer timescales become more noticeable, in which case the PV increases with τ.

We apply this algorithm to the time series of measurements of Ca II H&K and Hα indices. We complement this analysis using also the V-band photometry collected in the EXORAP survey. In general, for each star we find that the PV diagrams of the three proxies look alike (see Fig. 1 for an example): they generally increase at small timescales τ; they reach a plateau at roughly 10–40 days, and then increase to level off again at $\tau \gtrsim 50$ days. Our interpretation of these diagrams is that the first plateau corresponds to the stellar rotation period, consistently to the GLS analysis. The second flattening is likely related to the growth and decay of chromospheric ARs, as also suggested by Donahue et al.(1997a) and Donahue et al.(1997b). Our results are consistent with other analysis of M dwarfs, which indicate that ARs of main sequence M dwarfs evolve with timescales of ∼100 days (Davenport et al. 2015; Robertson et al. 2015; Newton et al. 2016).

In Fig. 2 we plot the relationship between the stellar rotation and the X-ray luminosity for M stars. In particular we compare the sample of M dwarfs analyzed by Pizzolato et al.(2003) with our sample of stars, divided into two subsamples depending on stellar effective temperature. The former are in the saturated regime, i.e. the L_X/L_{bol} ratio is

maximum and does not depend on the rotation period. These stars are typically more active than ours, for which we find that the X-ray luminosity decreases with increasing rotation period (i.e. stars in our sample are in the non-saturated regime). Moreover, we find that the locus occupied in the diagram moves to the right side as the effective temperature (and the stellar mass) decreases. If we assume that the X-ray saturation level (the horizontal dashed-dotted line in the plot) does not depend on stellar mass, then this suggests that the saturation level is reached at increasing stellar rotation as stellar mass decreases. This behavior, across all mass bins, is shown in the right panel of Fig. 2, where we show the collection of all best-fit relations found by Pizzolato et al. (2003) together with the new relations found in our analysis.

4. Flux-flux relationships

For each star in our sample we compute the average excess flux for each chromospheric line. Fig. 3 shows the comparison between pairs of fluxes. Several samples from literature are overplotted for comparison: a sample of F, G, and K stars from López-Santiago et al. (2010), Martínez-Arnáiz et al. (2010), Martínez-Arnáiz et al. (2011), a sample of late-K and M dwarfs (from the same authors), and a sample of pre-MS M stars from Stelzer et al. (2013).

Our sample of M dwarfs seems to follow the same trend as FGK stars and other late-K/early-M dwarfs for the Ca II H&K doublet, for pairs of Balmer lines and for the Ca II K vs. Hα relationship without any obvious deviation between samples.

In Fig. 4 we show the averaged Ca II K vs. Hα relationship in linear scale, where for each star the error bars represent the scatter of the time series of measurements around the median value. We find that the trend is not monotonic: the flux radiated in the Hα line initially decreases with increasing Ca II H&K excess flux, reaches a minimum, and finally increases with the Ca II H&K flux.

Previous observational studies performed on similar samples of stars (K- and M-type main sequence stars, e.g., Stauffer & Hartmann. 1986, Giampapa et al. 1989, Robinson et al. 1990, Rauscher & Marcy 2006, Walcowicz & Hawley 2009) have found comparable results. This evidence has been also supported by chromospheric models (Cram & Mullan 1979, Cram et al. 1987, Rutten et al. 1989, Houdebine et al. 1995, Houdebine & Stempels 1997), according to which the chromospheric Ca II H&K emission lines are collisionally dominated while the Hα line is radiation-dominated. With these assumptions, the Ca II H&K flux steadily increases with pressure, while the increase of the optical depth initially leads to a deeper absorption profile in the Hα line. This trend is reverted as

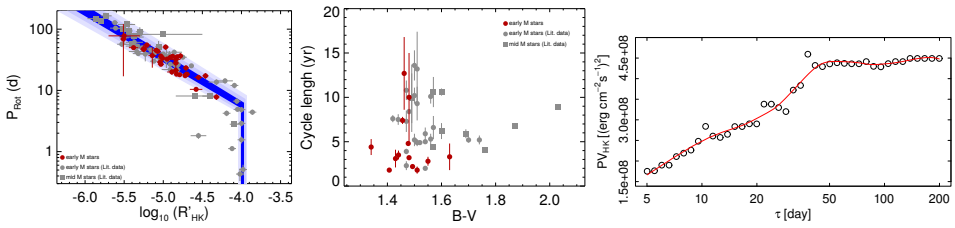

Figure 1. *Left panel* - Rotation periods in our stellar samples (red dots) as a function of the R'_{HK} activity proxy. Gray symbols mark other published samples of main sequence M dwarfs. *Middle panel* - Cycle length as a function of B-V color. Symbols are the same as in the left panel. *Central panel* - Activity cycle length vs. B-V colors for different samples of M dwarfs. *Right panel* - Example of the PV analysis showing the stellar rotation period (the flattening at ∼15 days) and the ARs lifetime (the flattening at ∼50 days).

soon as the electron density is high enough to take the Hα line into the collisionally dominated formation regime, leading to the fill-in of the line.

In Fig. 4 we also show the Ca II K vs. Hα relationship for each star using the bestfit line of the corresponding data, and we show the correlation between the slope of these bestfit lines with the stellar effective temperature. We find evidence of decreasing steepness of the flux-flux relationship with increasing effective stellar temperature with a confidence level of $\sim$4%. Stelzer et al. (2013) found a similar trend by analyzing a sample of pre-MS low-mass stars in the 2500–4500 K temperature range.

Meunier & Delfosse 2009 already analyzed the F_{HK} vs. $F_{H\alpha}$ relationship for the Sun. In particular, they use spatially resolved observations of the solar surface covering 1.5 activity cycles, and find that the presence of dark filaments affects the correlation between F_{HK} and $F_{H\alpha}$ on daily-to-weekly timescales, eventually leading to negative correlations. Moreover, for a fixed contrast of Hα plages on the solar disk, the slope of the F_{HK} vs. $F_{H\alpha}$ relationship tends to decrease with increasing contrast of the filaments. This is due to the fact that solar filaments are optically thicker in the Hα than in the Ca II H&K lines. Thus, the increase in slope with decreasing effective temperature that we find may indicate that the Hα absorption in equivalent active regions decreases towards later M types.

We draw the same conclusion analyzing the ratio between Hα and Hβ fluxes, which is an indicator of the physical conditions of the emitting regions (e.g. Landman & Mongillo 1979; Chester 1991). Fig. 5 shows the Balmer decrement $F_{H\alpha}/F_{H\beta}$ as a function of the effective temperature, together with solar plages and prominences for comparison. The stars in our sample show a decreasing trend in Balmer decrement towards later spectral types. Once again, stars in the spectral range between M0 and M1.5 are compatible with a filament-dominated scenario, while chromospheres of later spectral type stars are dominated by plages. This statement is also consistent with pre-MS M stars (Stelzer et al. 2013) and the active M dwarf templates from the Sloan Digital Sky Survey (Bochanski et al. 2007).

In addition to the flux-flux relationships between different chromospheric activity indicators, we also studied the chromospheric-coronal relation. Our sample of M dwarfs seems to follow the same trend as other literature stellar samples and extend it towards lower activity levels (Fig. 6).

5. Summary

In the context of the HADES project, we collected optical spectroscopy and photometry for a sample of 71 low-activity early-M dwarfs, and complemented our data with the X-ray fluxes reported in public data archives. In this contribution I have summarized the main

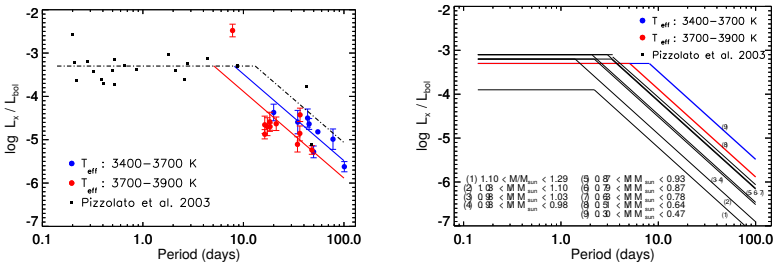

Figure 2. *Left panel* - L_X/L_{bol} vs. stellar rotation for different samples of M dwarfs. *Right panel* - L_X/L_{bol} vs. stellar rotation loci for different samples of main sequence stars.

results of a series of papers reporting our analysis (Maldonado et al. 2017; Scandariato et al. 2017; Suárez Mascareño et al. 2018; González-Álvarez et al. 2019).

The M dwarfs in our sample have rotation periods of the order of 20–100 days which are well correlated with the R'_{HK} activity indicators. Comparing the rotation periods with the X-ray fluxes, we argue that early-M dwarfs with rotation periods of 7–10 days are already saturated and the fluxes increase with decreasing stellar mass. We also detect activity cycles of a few years, but this result is biased by the fact that our time series are 6.5 years long, hence we fail to detect longer cycles. Finally, we find evidence that ARs evolve in a few stellar rotations. In this perspective, we find that low-activity M dwarfs are similar to other stellar samples in literature.

Our analysis of the activity proxies extends the chromospheric and coronal flux-flux relationships of samples of active/young stars towards lower activity levels. We also find evidence that at very low activity levels, and at earlier M spectral types, the chromosphere is dominated by cold filaments absorbing in the Hα, while at higher activity levels, and in general at later M types, the emission by plages dominates.

References

Affer, L., Micela, G., Damasso, M., et al. 2016, *A&A*, 593, A117
Bochanski, J. J., West, A. A., Hawley, S. L., et al. 2007, *AJ*, 133, 531
Cosentino, R., Lovis, C., Pepe, F., et al. 2012, *Proc. SPIE*, 8446, 84461V
Chester, M. M. 1991, Ph.D. Thesis
Covino, E., Esposito, M., Barbieri, M., et al. 2013, *A&A*, 554, A28
Cram, L. E., & Mullan, D. J. 1979, *ApJ*, 234, 579
Cram, L. E., & Giampapa, M. S. 1987, *ApJ*, 323, 316
Davenport, J. R. A., Hebb, L., & Hawley, S. L. 2015, *ApJ*, 806, 212
Donahue, R. A., Dobson, A. K., & Baliunas, S. L. 1997, *Solar Phys.*, 171, 211

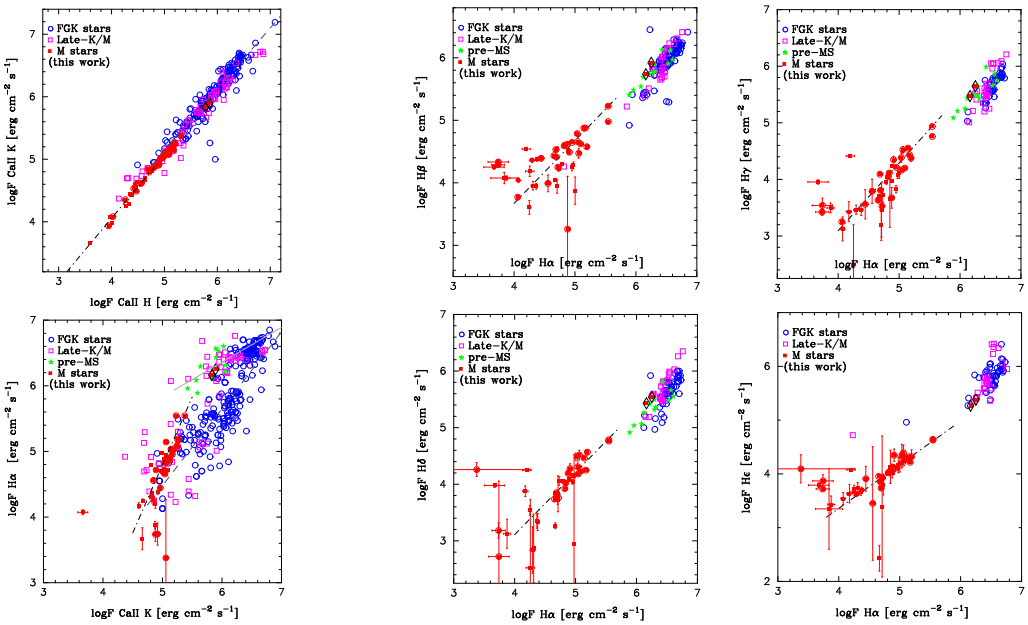

Figure 3. *Left column* - Correlations between Ca II H&K and Hα fluxes. *Central and right columns* - Correlations between the Balmer lines in the analyzed spectra. For the sake of comparison, in all plots we show other stellar samples from the studies discussed in the text.

Donahue, R. A., Dobson, A. K., & Baliunas, S. L. 1997, *Solar Phys.*, 171, 191
Giampapa, M. S., Cram, L. E., & Wild, W. J. 1989, *ApJ*, 345, 536
González-Álvarez, E., Micela, G., Maldonado, J., et al. 2019, *A&A*, 624, A27
Henry, T. J., Jao, W.-C., Subasavage, J. P., et al. 2006, *AJ*, 132, 2360
Houdebine, E. R., Doyle, J. G., & Koscielecki, M. 1995, *A&A*, 294, 773
Houdebine, E. R., & Stempels, H. C. 1997, *A&A*, 326, 1143
Landman, D. A., & Mongillo, M. 1979, *ApJ*, 230, 581
López-Santiago, J., Montes, D., Gálvez-Ortiz, M. C., et al. 2010, *A&A*, 514, A97
Lovis, C., & Pepe, F. 2007, *A&A*, 468, 1115
Maldonado, J., Scandariato, G., Stelzer, B., et al. 2017, *A&A*, 598, A27
Martínez-Arnáiz, R., Maldonado, J., Montes, D., et al. 2010, *A&A*, 520, A79
Martínez-Arnáiz, R., López-Santiago, J., Crespo-Chacón, I., et al. 2011, *MNRAS*, 414, 2629
Newton, E. R., Irwin, J., Charbonneau, D., et al. 2016, *ApJ*, 821, 93
Perger, M., García-Piquer, A., Ribas, I., et al. 2017, *A&A*, 598, A26
Pizzolato, N., Maggio, A., Micela, G., et al. 2003, *A&A*, 397, 147
Rauscher, E., & Marcy, G. W. 2006, *PASP*, 118, 617
Reid, I. N., Gizis, J. E., & Hawley, S. L. 2002, *AJ*, 124, 2721
Robertson, P., Endl, M., Henry, G. W., et al. 2015, *ApJ*, 801, 79
Robinson, R. D., Cram, L. E., & Giampapa, M. S. 1990, *ApJS*, 74, 891
Rutten, R. G. M., Zwaan, C., Schrijver, C. J., Duncan, D. K., & Mewe, R. 1989, *A&A*, 219, 239
Scandariato, G., Maldonado, J., Affer, L., et al. 2017, *A&A*, 598, A28
Stauffer, J. R., & Hartmann, L. W. 1986, *Cool Stars, Stellar Systems and the Sun*, 254, 58
Stelzer, B., Frasca, A., Alcalá, J. M., et al. 2013, *A&A*, 558, A141
Suárez Mascareño, A., Rebolo, R., González Hernández, J. I., et al. 2018, *A&A*, 612, A89
Vidotto, A. A., Jardine, M., Morin, J., et al. 2013, *A&A*, 557, A67
Walkowicz, L. M., & Hawley, S. L. 2009, *AJ*, 137, 3297
Zechmeister, M., & Kürster, M. 2009, *A&A*, 496, 577

Discussion

KOSOVICHEV: Is Hα always the emission line?

SCANDARIATO: No, it isn't. As our sample of stars is biased towards low activity levels, the Hα line is most often in absorption. This line seems to have a tricky behavior, as it is not filled in as the chromospheric activity increases. As a matter of fact, when we subtract the reference template, the residuals show an extra-absorption in the Hα, before emission comes into play leading the residuals to show a flux excess in the core of the line.

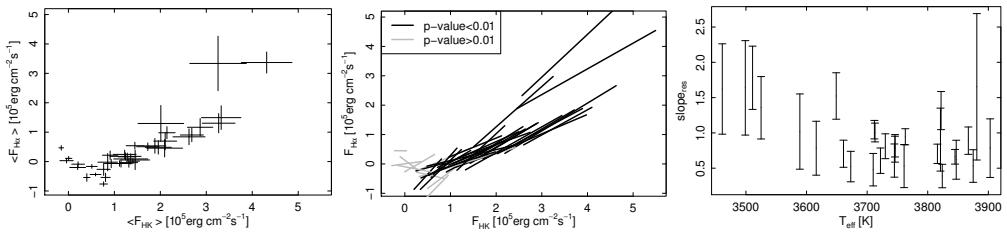

Figure 4. *Left panel* - Correlations between Ca II H&K doublet and Hα fluxes in linear scale. Error bars represent the scatter of the measurements in the time series. *Central panel* - Same as in the left panel, but representing each star as the linear best fit of the time series of measurements. The *p-values* of the correlation tests are also reported. *Right panel* - The slope of the linear best fits in black in the central panel as a function of stellar effective temperature.

HAN: Maybe I have missed something, but how did you get the rotational period? You are using L-S approach from variations of radial velocities?

SCANDARIATO: We use the time series of the broad-band photometry and the chromospheric proxies, and we apply the L-S approach to them. Radial velocities are not used to measure the stellar rotation in the works discussed in my talk.

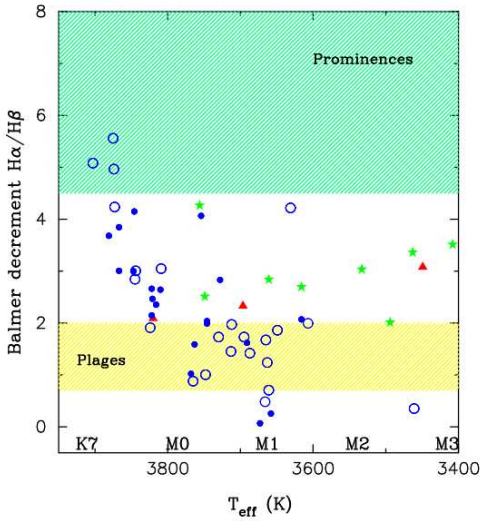

Figure 5. Balmer decrement $F_{H\alpha}/F_{H\beta}$ vs. the effective temperature. Stars in our sample are marked as circles. Green stars and red triangles mark the samples of Stelzer et al. (2013) and Bochanski et al. (2007) respectively. Typical ranges of solar plages and prominences are shown as hatched areas.

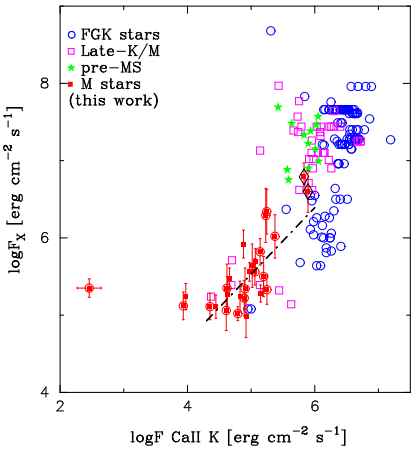

Figure 6. X-ray flux vs. Ca II K. Symbols are the same as in Fig. 3.